Temporal Variability in Water Quality and Phytoplankton Biomass in a Low-Inflow Estuary (Baffin Bay, TX)

Laura Beecraft[1] · Michael S. Wetz[1]

Abstract

Low-inflow estuaries are subject to inconsistent seasonal and interannual variability in precipitation and watershed influences on hydrology, complicating understanding and prediction of water quality and phytoplankton dynamics. We quantified variability in environmental conditions and phytoplankton biomass over an 8-year period in a eutrophying lagoonal estuary (Baffin Bay, Texas) that experiences prolonged low inflow conditions punctuated by episodic high inflow events, resulting in a large interannual salinity range (20–62 in this study). Using a 90th percentile threshold of chlorophyll *a* concentration to classify blooms, we observed a higher frequency of blooms at high salinity conditions (20% of high salinity observations were blooms) compared to intermediate (5%) and low (6%) salinity. The conditions and composition of blooms varied at different salinities, with blooms at high salinities dominated by the ecologically damaging "brown tide" *Aureoumbra lagunensis*, whereas lower salinity blooms were dominated by a variety of phytoplankton groups. The distinct bloom communities that developed under different salinities suggest that complex drivers of community dynamics are at play in Baffin Bay and provide insight into what we can anticipate during future periods of prolonged drought, as well as following sporadic heavy rainfall events, both of which are expected to increase in frequency with climate change.

Keywords Lagoon · Salinity · Nutrients · Residence time · Bloom

Introduction

Estuaries are dynamic systems with strong environmental gradients, and often have disproportionately large ecological and human-associated value relative to their size (Pendleton 2010; Barbier et al. 2011). Low-inflow estuaries and lagoons are characterized by minimal freshwater inflow for extended periods, limited ocean-connectivity, shallow depth, and are commonly located in subtropical regions that are subjected to arid or semiarid conditions (Largier 2010). Consequently, they are often poorly flushed and evidence is emerging that these types of estuaries may be particularly susceptible to eutrophication (Bricker et al. 2008; Scavia and Liu 2009).

Baffin Bay is a subtropical lagoon located on the south Texas (USA) coast and is part of the Laguna Madre estuary complex. It receives low base freshwater inflow and has no direct connection to the Gulf of Mexico, resulting in frequent hypersaline conditions and long residence times (> 1 year on average) (Wetz et al. 2017; Montagna et al. 2018). Prolonged dry periods in south Texas can last upwards of 5 years, and salinities in the bay can exceed 70 during these times (Tolan 2007). However, episodic high rainfall periods also occur often during El Niño years, resulting in reduced salinities and decreasing residence time to several weeks–months (Cira et al. 2021).

During multi-year dry periods that have occurred from 1989 to present, Baffin Bay and Laguna Madre have experienced harmful "brown tides" of the phytoplankton *Aureoumbra lagunensis* (e.g. Buskey et al. 2001; Cotner et al. 2004; Cira and Wetz 2019). *A. lagunensis* forms near-monospecific blooms, with negative consequences for the ecosystem as well as ecosystem services (Buskey and Hyatt 1995; Onuf 1996; Street et al. 1997). Although Baffin Bay generally receives low inflow, sporadic high inflow events may bring increased land-based nutrient

✉ Laura Beecraft
    Laura.beecraft@tamucc.edu

    Michael S. Wetz
    Michael.Wetz@tamucc.edu

[1] Harte Research Institute for Gulf of Mexico Studies, 6300 Ocean Drive, Unit 5869, Corpus Christi, TX 78412, USA

and sediment loads into the system, along with dramatic changes to salinity in a short time-period. Without a connection to the ocean however, nutrients brought into the system are likely to be retained for long periods of time and make it more susceptible to eutrophication. Indeed, multiple lines of evidence suggest that Baffin Bay is undergoing eutrophication, including high and increasing nutrient or chlorophyll levels over the past 3–4 decades (Wetz et al. 2017; Bugica et al. 2020) and recent tracer studies documenting a significant signature of human-derived nutrients (D. Felix, unpubl. data).

In the future, projections suggest that global climate change may lead to warmer temperatures, increased evaporation, and decreased average precipitation on the South Texas coast where Baffin Bay is located (Seneviratne et al. 2012). Consequently, freshwater inflows are expected to be lower as well (Kloesel et al. 2018; Nielsen-Gammon et al. 2022). Reduced inflow may exacerbate hypersalinity conditions and further increase residence times. Other subtropical regions around the globe with low-inflow estuaries are expected to see similar climatic changes, including South Africa, the Mediterranean, and Australia, for example (Seneviratne et al. 2012; Leterme et al. 2015; Scanes et al. 2020). Despite projections of an overall drying trend, storm events are predicted to be more severe on the South Texas coast (Seneviratne et al. 2012; Kloesel et al. 2018).

There is a need to understand the conditions that trigger phytoplankton bloom development in low-inflow estuaries, especially given that they appear to be susceptible to eutrophication and expectations of climate-induced hydrologic changes. Phytoplankton blooms are controlled by site-specific variability of factors influencing phytoplankton growth – and conditions producing increased biomass are not consistent across estuaries, or even over time in the same estuary (e.g. Brito et al. 2012; Carstensen et al. 2015). Low inflow and long residence times produce conditions that can limit (lack of a constant supply of river-derived nutrients) or promote (long residence time, nutrient retention, and recycling) phytoplankton growth. Understanding the conditions leading to high biomass, harmful algal blooms, and water quality issues is critical for land and water management stakeholders to mitigate potential negative impacts on the living resources and ecosystem services that estuaries support.

In the present study, we examined 8 years of monthly monitoring data from Baffin Bay to better understand the timing and drivers of phytoplankton blooms. Specific objectives were to (i) quantify temporal trends in environmental conditions and phytoplankton abundance and (ii) quantify the frequency of phytoplankton bloom events (based on chlorophyll a (Chl a) concentration) under various hydrologic regimes to elucidate the conditions associated with their development and demise.

Methods

Site Characteristics

Baffin Bay is a shallow (mean depth of 2.3 m) tributary of the Laguna Madre, connecting at its mouth with the Upper Laguna Madre to the east (Fig. 1). Watershed land use coverage for Baffin Bay is dominated by agriculture (primarily cotton farming; 44%), followed by scrub (35%) and grassland (8%) (NOAA Coastal Change Assessment Program). In comparison, human development is relatively limited within the watershed, with the city of Kingsville being the largest populated area (pop. 25,367). Winds can be relatively strong in the region and are thought to play a dominant role in hydrology of the system, with the water column generally being well mixed throughout much of the year (Tunnell and Judd 2002). The nearest inlets that allow for exchange between the Laguna Madre and Gulf of Mexico are Packery Channel (~41 km north of Baffin Bay), Aransas Pass (~70 km north of Baffin Bay), and Port Mansfield (~80 km south of Baffin Bay). These distances, along with diurnal tidal ranges of only 2–3 cm, result in minimal overall tidal influence on the system.

Field Measurements

This study uses data from six sites in Baffin Bay (Fig. 1) sampled monthly from May 2013 to December 2021. These sites were selected to provide representative spatial coverage of Baffin Bay, including the three secondary bays with different inflow sources (sites BB1, BB2, BB5), and extending along the main channel of the bay to its connection with the Laguna Madre (sites BB3, BB4, BB6). At each site, water depth, Secchi depth, and vertical profiles of temperature, salinity, conductivity, pH, and dissolved oxygen (DO) were conducted using a Professional Plus YSI multiparameter sonde (YSI, Yellow Springs, OH), calibrated within 24 h of sample collection. A salinity stratification coefficient was estimated by subtracting surface (0.1 m) from near-bottom salinity. Salinity is the dominant component of density stratification in Baffin Bay, which tends to only occur episodically in summer-fall, owing to the persistent high winds in the area (Wetz, unpubl. data). Surface water (0.1 m) was collected using a Van Dorn sampler and transferred to rinsed, acid-washed brown HDPE bottles: a 1-L bottle was stored on ice for subsequent nutrient, carbon, and Chl a analysis, and a 500-mL bottle was stored at ambient temperature for phytoplankton enumeration.

Water Chemistry and Phytoplankton Analyses

Upon return to the laboratory, sample bottles were gently mixed and two 50 mL subsamples were filtered through combusted 25 mm GF/F (0.7 μm) filters and stored frozen (−20
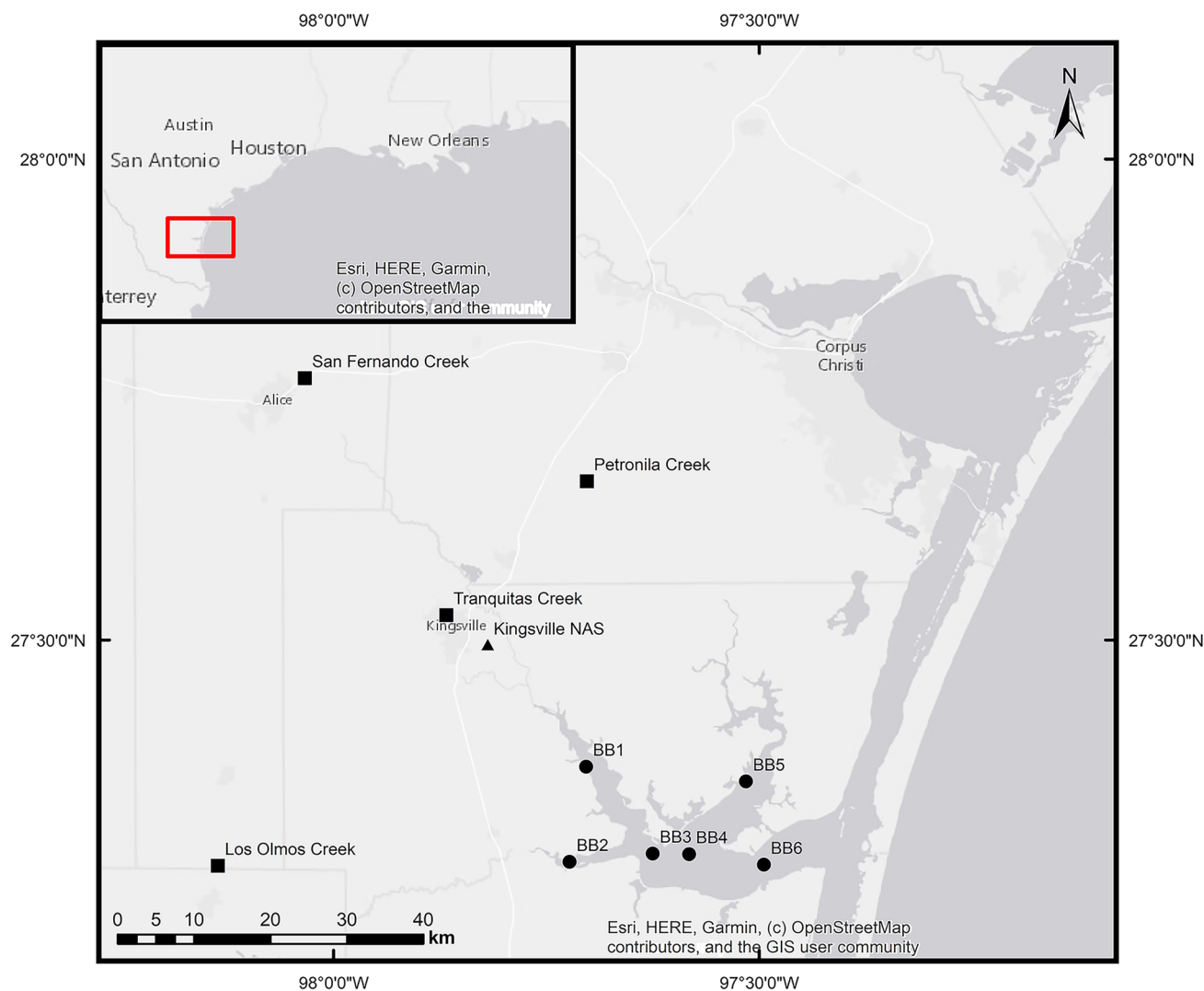
Fig. 1 Map showing the location of Baffin Bay, TX, in the northwestern Gulf of Mexico (inset) and of the bay. Circles indicate the six monthly sampling stations in Baffin Bay; black squares are the USGS NWIS gauge stations used for inflow data to Baffin Bay, and the triangle is the Kingsville NAS, TX, station used for meteorological data sourced from NOAA

°C) until analysis for inorganic nutrients (silicate, orthophosphate, ammonium, nitrite, and nitrate (NO_x)), total dissolved nitrogen (TDN) and dissolved organic carbon (DOC), and total dissolved phosphorus (TDP), respectively (refer to Wetz et al. 2017, for full details). Dissolved inorganic nitrogen (DIN) was calculated as ($NH_4 + NO_2 + NO_3$), dissolved organic nitrogen (DON) as TDN–DIN, and dissolved organic phosphorus (DOP) as (TDP–orthophosphate). 50 mL subsamples of whole water were collected for total organic carbon (TOC) and total nitrogen (TN) and stored frozen until analysis. After thawing to room temperature, inorganic nutrients were analyzed on a Seal QuAAtro autoanalyzer. DOC, TOC, TDN, and TN were analyzed using the high-temperature catalytic oxidation method on a Shimadzu TOC-Vs analyzer with

nitrogen module. TP and TDP were analyzed using persulfate digestion prior to measurement as orthophosphate.

Duplicate Chl *a* samples were collected by filtering known volumes of sample water on 25 mm Whatman GF/F filters at low vacuum pressure (< 5 mm Hg) and stored frozen (−20 °C) until analysis. Chl *a* was extracted passively in 90% acetone for 16–24 h, without acidification, and quantified fluorometrically using a Turner Trilogy fluorometer. Estimates of the dominant phytoplankton functional groups observed during bloom events were obtained from Cira et al. (2021) and Chin et al. (2022), and supplemented with microscopic counts using the Utermöhl method where data was otherwise not available (see Cira et al. 2021 for detailed methods).

Meteorological Data

Local meteorological data for the Kingsville NAS, TX, was obtained from the NOAA National Centers for Environmental Information (NCEI) Local Climatological Data (LCD) source. Discharge data were obtained from USGS National Water Information System (NWIS) for the creeks flowing into Baffin Bay: San Fernando (USGS Gauge Station 8211900), Tranquintas (8212300), Los Olmos (8212400), and Petronila (8212820). Data from Petronila Creek was not available for the full study period (available 2018–06-07 to 2022–03-11). ONI (Oceanic Niño Index) values were obtained from the NOAA National Weather Service Climate Prediction Center (http://www.cpc.ncep.noaa.gov). Rolling multi-day averages of discharge and wind-speed were calculated for the periods preceding our sampling dates.

Classification of Salinity and Chlorophyll Observations

Observations were categorized as low, intermediate, or high salinity by comparing values to the 25th (31.9) and 75th (49.5) percentiles of observed surface water salinities over the study period: < 25th percentile = low, 25th–75th = intermediate, > 75th percentile = high. ONI values were used to categorize sampling years as El Niño (index ≥ 0.5), La Niña (≤ -0.5), or neutral (-0.5–0.5) (Table S2). The 90th percentile (calculated from log-transformed data due to the log-normal distribution of Chl *a* concentrations) of observed Chl *a* concentrations over the duration of the study period was used to categorize observations as bloom ($\geq$ 90th percentile) and non-bloom concentrations.

Statistical Analyses

For samples when nutrient concentrations were below the limit of detection (LOD), but present, 0.5*LOD was used as a conservative estimate of concentrations which were unlikely to be precisely 0 but could not be accurately quantified by the analysis method (LODs: ammonium 0.03 μM; $NO_2 + NO_3$ 0.02 μM; orthophosphate 0.01 μM; silicate 0.01 μM).

Environmental conditions were compared among the three salinity categories by one-way analysis of variance (ANOVA). Welch's ANOVA for unequal variance was used for variables when Bartlett's test indicated unequal variance among groups, followed by Games-Howell post hoc pairwise comparisons to adjust for unequal sample numbers and variance among groups. Spearman rank correlation analyses were performed to compare responses among different environmental and water chemistry variables. Principal components analysis (PCA) was used to visualize patterns among samples with respect to environmental and water quality variables, applying a natural log ($\ln(x + 1)$) transformation

Fig. 2 **a** Daily precipitation measured at the Kingsville NAS, TX, ▶ from NOAA LCD. **b** Instantaneous discharge into Baffin Bay over time, summarized from USGS NWIS gauge data for 4 inflow streams (grey region-data unavailable for Petronila preceding 2018–06-07). **c** Surface water salinity over time, measured during monthly sampling events at six sites within Baffin Bay. Horizontal lines indicate median (solid line), 25th and 75th percentiles (dashed lines) salinities for the complete sampling period, used to categorize observations as "high," "intermediate," or "low" salinity

to variables where appropriate, prior to calculation of the correlation cross products matrix. Statistical analyses were performed and accompanying figures produced using PC-ORD Version 7.08 (McCune and Mefford 2018) and R version 4.1.0 (R Core Team 2020) and additional packages (Kassambara 2020; Wickham et al. 2019). Environmental and water quality data are available through the GRIIDC Data Repository (Table S1).

Results

Freshwater inflow displayed large interannual variation (Fig. 2), reaching over 80 and 60 $m^3 \cdot s^{-1}$ in 2018 and 2021, respectively, while the mean daily inflow averaged across sampling years was below 1 $m^3 \cdot s^{-1}$ (Table S3). Salinity responded inversely to inflow, decreasing quickly following inflow events, and gradually increasing during extended periods of low inflow (Fig. 2). Mean annual salinities were lowest in 2015 (28.2) and 2021 (29.5) and highest in 2013 (61.8) (Table S3). Precipitation data recorded at Kingsville NAS corresponded to inflow patterns in some cases, but also explained changes in salinity that were not captured by the available inflow data, such as decreasing salinity in the second half of 2014.

Chl *a* concentrations displayed large spatio-temporal variation, with individual observations ranging from 1.2 to 74 $\mu g \cdot L^{-1}$ during the study period, and annual means from 11.2 (2017) to 31.3 $\mu g \cdot L^{-1}$ (2013) (Fig. 3; Table S3). Nutrient concentrations were also dynamic, and interestingly, neither nutrient nor Chl *a* concentrations showed consistently co-occurring changes with inflow or each other (Figs. 2, 3, S1, S2, S3). For example, silicate and orthophosphate concentrations had inverse relationships with salinity below ca. 30 (Figs. S1, S3), suggesting inflow and watershed sources – but this trend was not consistent across the observed salinity gradient and did not show a pattern with Chl *a*. A higher proportion of "bloom" Chl *a* concentrations (> 33.8 $\mu g \cdot L^{-1}$) was observed at high compared to intermediate and low salinity conditions (20, 5, and 6% respectively; Table 1; Fig. 3). Maximum observed concentrations occurred during low salinity periods in 2015 and 2019 (74.4, 62.8 $\mu g \cdot L^{-1}$, respectively). Chl *a* concentrations were lower at intermediate salinities compared to high and low, consistent with the
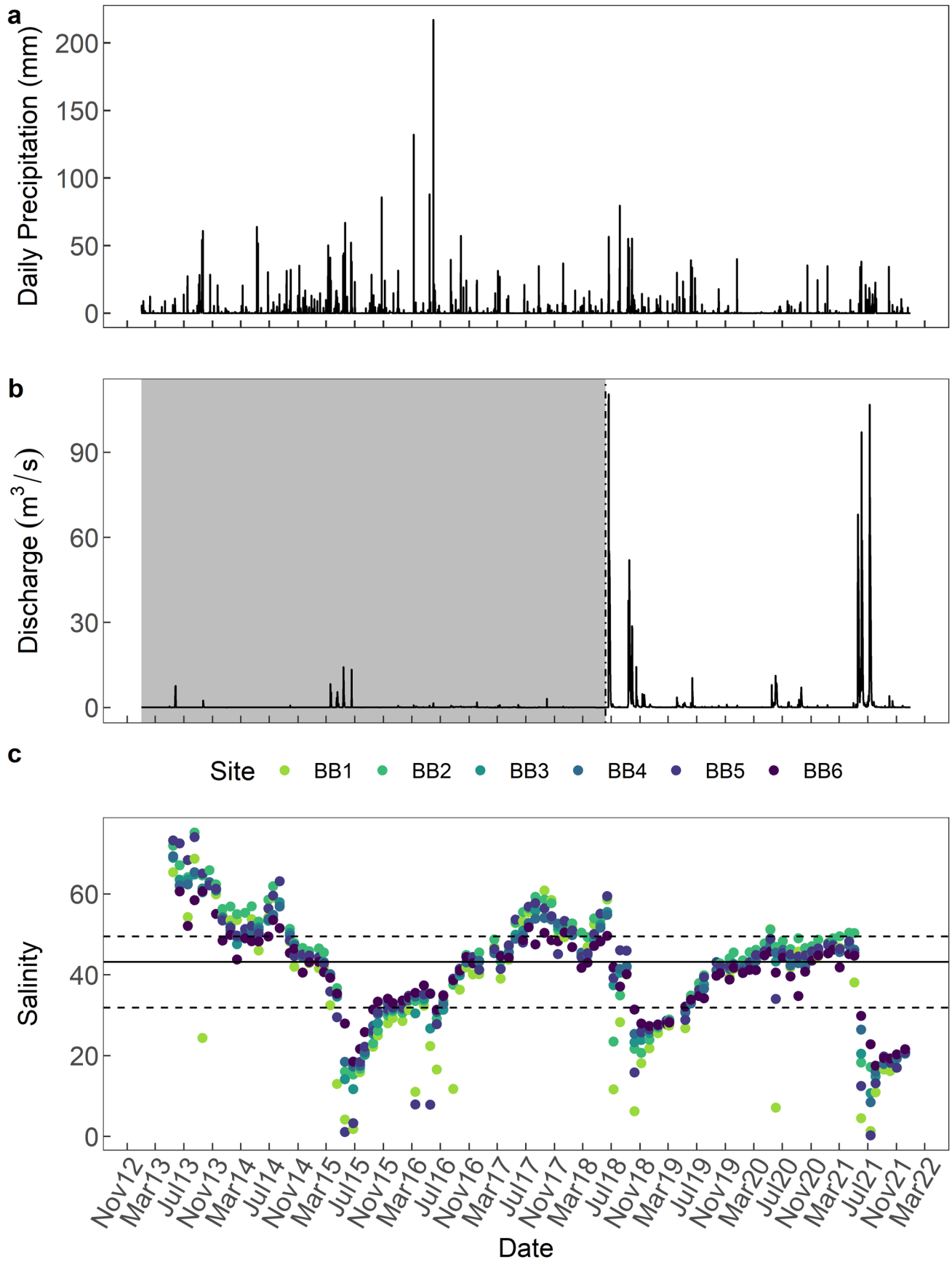
Fig. 3 a Surface water Chl *a* concentration for six sites within Baffin Bay (points), and average Chl *a* concentration for the bay (solid line), over time. The dashed horizontal line indicates the 90th percentile of Chl *a* concentrations for the complete sampling period (33.8 μg·L^{-1}), used to categorize observations as "bloom" or "non-bloom." **b** Bay-wide (average of 6 sites) concentrations of total nitrogen (TN), total dissolved nitrogen (TDN), and dissolved organic nitrogen (DON) concentrations over time
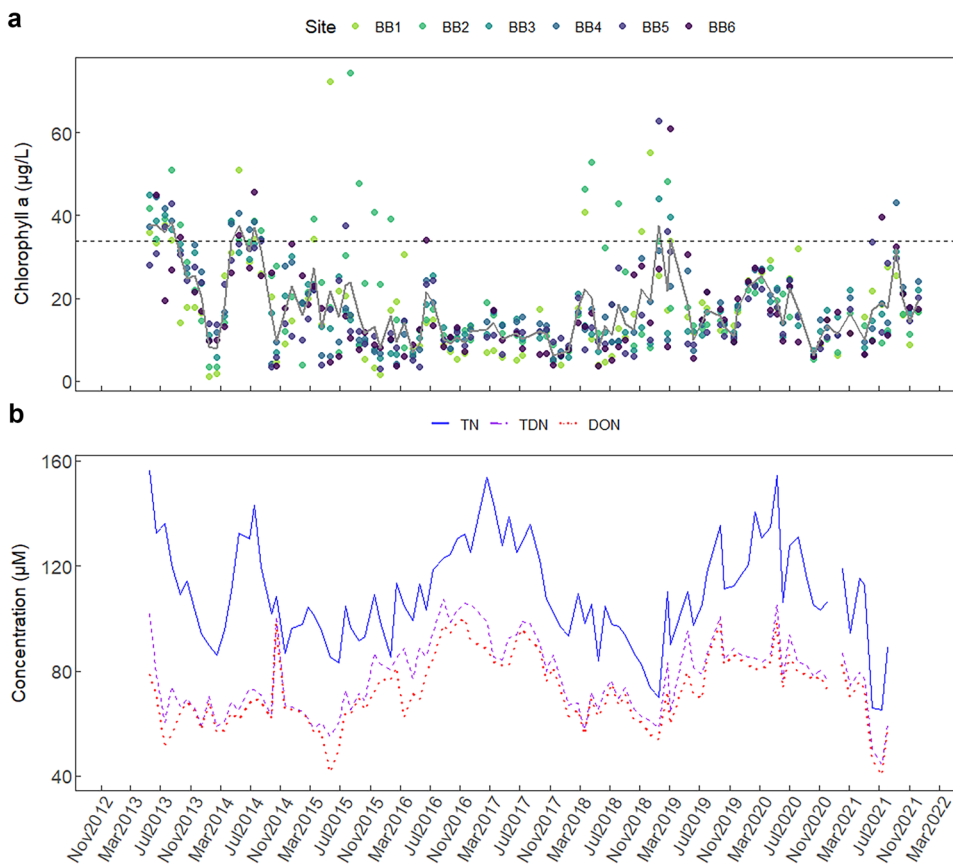
observed bloom frequency (averages of 21.7, 14.7 and 19.7 μg·L^{-1} at high, intermediate, and low salinities, respectively) (Fig. 4; Tables S4, S5).

Ammonium, DIN, TP, DOP, and the ratio of DIN:DIP did not vary among salinity conditions. Ammonium was highest in 2016 and 2013 (annual means 6.98 and 4.73 μM; Table S3; Fig. S3). Mean annual TP and DOP were similar across sampling years, ranging from 2.2 to 3.8 μM and 0.77 to 1.42 μM, respectively, and both lowest in 2013. DON was highest at intermediate salinities (77.4 μM ± 15.1), followed by high (71.4 μM ± 15.3) and low (61.7 μM ± 14.6) salinity conditions, with the highest annual means in 2017 and 2016 (Fig. 3; Table S3). Silicate was lower at high (85.7 μM ± 23.6) compared to intermediate

Table 1 Frequency of bloom (≥ 33.8 μg·L^{-1}) and non-bloom Chl *a* concentrations observed at high (> 49.5), intermediate, and low (< 31.9) salinities from 2013 to 2021 (Supplementary Materials Table S2 for details by year)

Salinity category	Bloom	Non-bloom	Percentage bloom
Dry	36	146	20%
Intermediate	15	265	5%
Wet	9	135	6%

(107.3 μM ± 39.4) and low (108.4 μM ± 87.3) salinities; highest annual means were observed at the end of the study period, 2021 and 2020 (165.9 and 131.4 μM, respectively). NO$_x$ concentrations were higher at low compared to intermediate salinities (mean: high 1.2, intermediate 0.8, low 2 μM). Mean annual NO$_x$ was highest in 2013 (2.94 μM); however, the median annual value was highest in 2018. Orthophosphate was higher at low salinity conditions (mean: high 0.5, intermediate 0.4, low 1.3 μM), although this did not result in any significant differences in the ratio of DIN:DIP among salinity conditions (Fig. 4; Tables S4, S5). Spearman rank correlation analysis produced significant correlations among many response variables (*p*-value < 0.05; Table S6). However, correlation coefficients were generally low and visual examination of the plots (Figs. S1, S2) did not suggest strong relationships among responses. For example, the largest correlation coefficient with Chl *a* was TN ($r_s = 0.299$, $p << 0.05$; Fig. S2).

PCA of environmental and water quality conditions showed grouping in ordination space relating to salinity condition (Fig. 5). Axis 1 explained 19.6% of the variation in the cross-products matrix calculated from the environmental response variables (Table S7) and correlates most strongly with orthophosphate, as well as TDP, salinity and inflow. Axis 2 explained 16.2% of the variation and corresponds to
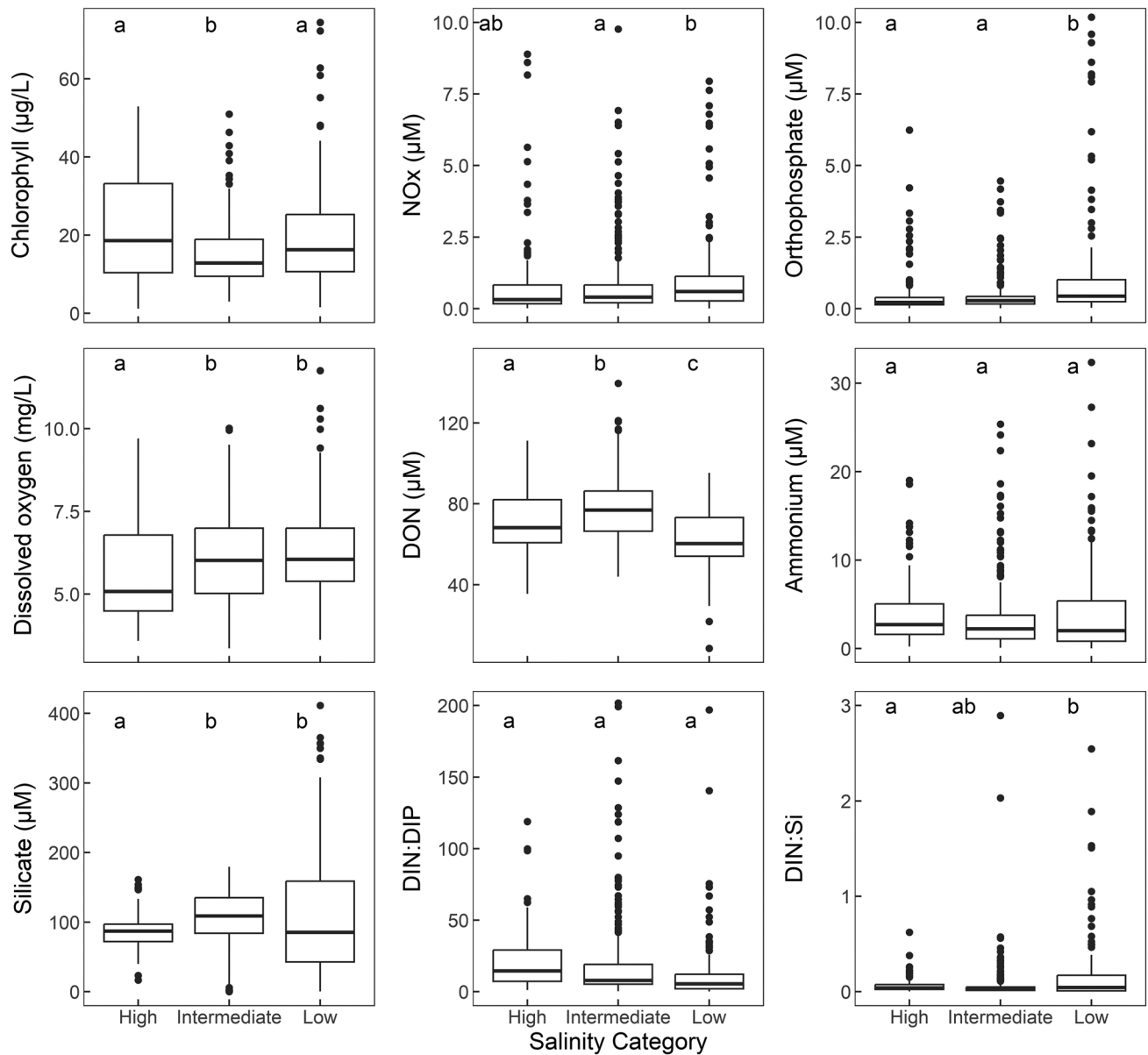
Fig. 4 Select environmental conditions at low, intermediate, and high salinity levels. Different letters indicate salinity levels/categories with significantly different conditions (based on one-way ANOVA or Welch's test based on variance among groups, and Games-Howell post hoc compari-son, $\alpha = 0.05$). Some outliers are excluded and y-axes reduced to better visualize the boxes. Complete results are available in Tables S4 and S5

organic and total nitrogen concentrations, as well as silicate, the ratio of DIN:Si, and Secchi depth (Fig. 5). High salinity observations, including blooms, showed the most similarity in ordination space. In addition to salinity, high salinity observations were positively associated with DON and TN and negatively with inorganic nitrogen and phosphorus concentrations and salinity stratification coefficients. Intermediate and low salinity observations – including the low salinity blooms – were more scattered in ordination space, indicating greater variability of environmental conditions associated with these observations. Low salinity observations were

generally associated with higher phosphorus concentrations as well as NO_x (Fig. 5).

The salinity stratification coefficient correlated with inflow in the PCA (Fig. 5) but did not have a significant Spearman correlation coefficient (Table S6). Salinity stratification coefficients ranged from −12 (BB5, 2014) to 38 (BB1, 2013), with most high coefficients occurring at sites BB1 and BB5 when surface water salinities were low. These observations did not consistently coincide with elevated Chl a. Secchi depth and Chl a varied among seasons (based on one-way ANOVA and post hoc pairwise
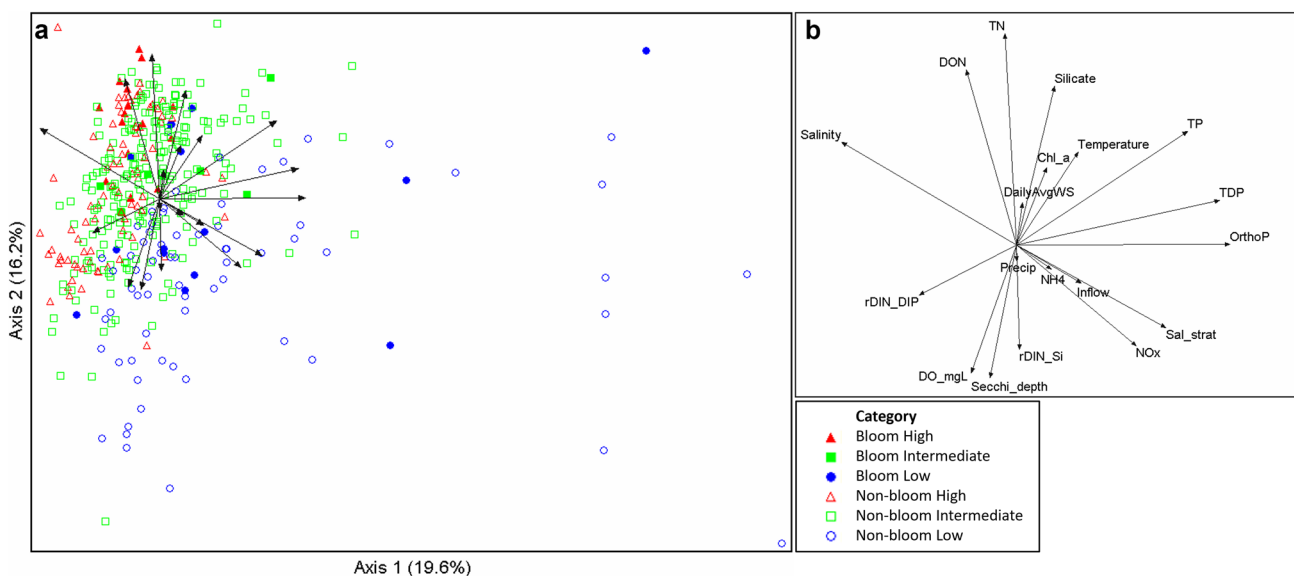
Fig. 5 Principal component analysis ordination plot of environmental and water chemistry parameters for sample dates from 2013 to 2020. Panel **a** symbology distinguishes between high (triangle), intermediate (square), and low (circle) salinity and bloom vs. non-bloom (filled vs. open symbols, respectively) dates/observations. Panel **b** shows the relative position of the environmental and water chemistry response variables

comparisons, results not shown): spring and summer Secchi depths were lower compared to fall and winter, and the reverse was true for Chl *a*. These differences were small in the case of Secchi depth, with mean and median values between 0.3 and 0.5 m, and Chl *a* seasonal means all fall

Fig. 6 Dominant (> 50% of biovolume) phytoplankton groups observed at bloom Chl *a* concentrations at high, intermediate, and low salinities

within the standard deviation of each other. Secchi depths also varied among sites, but Chl *a* did not.

There were clear differences in the phytoplankton group dominance of bloom observations at high, intermediate, and low salinities (Fig. 6). All the high salinity blooms during our study period were dominated (> 50% biovolume) by *A. lagunensis*. Blooms were dominated by a variety of groups at intermediate and low salinity, in particular diatoms, and sometimes euglenoids, dinoflagellates, or the photosynthetic ciliate *Mesodinium*. Blooms of *A. lagunensis* observed at intermediate and low salinities primarily occurred after a rain event at the end of a dry period.
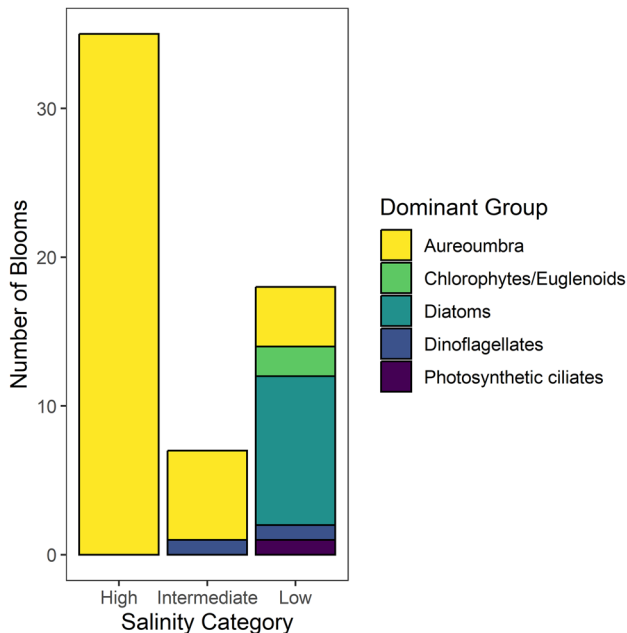
Discussion

Lagoonal, low-inflow estuaries are defined by a general lack of flushing and long residence times that make them susceptible to environmental stressors. Evidence is growing that points to their vulnerability to eutrophication and its associated symptoms such as persistent algal blooms and presence of harmful algal bloom-forming species (Knoppers et al. 1991; Bricker et al. 2003, 2008; Lemley et al. 2017, 2021). Thus, there is a need to understand the conditions that trigger phytoplankton bloom development, but relatively few studies exist from these types of estuaries compared to better studied river-influenced estuaries (Glibert et al. 2010; Barroso et al. 2018; Wilson et al. 2021). In the present study, we quantified phytoplankton bloom prevalence over an eight-year period in Baffin Bay, TX, a system that commonly experiences

prolonged dry periods followed by intermittent wet/flood periods, to better understand the timing and drivers of phytoplankton blooms. As discussed below, results show that the system is susceptible to phytoplankton blooms under both dry and wet conditions, although the character of blooms and their drivers vary.

There is no common definition for phytoplankton "blooms" (Smayda 1997), and system or context-specific approaches are commonly employed (Carstensen et al. 2007, 2015; Boyer et al. 2009; Pereira Coutinho et al. 2012). Generally, blooms constitute substantial biomass accumulation above background levels and the 90th percentile threshold used here (≥ 33.8 µg Chl $a \cdot L^{-1}$) provides a conservative reference for characterizing phytoplankton biomass over time and under different conditions in Baffin Bay. It is conservative in the sense that it is higher than concentrations considered to be eutrophic in freshwaters (U.S. EPA 2000), "screening levels" designated by the state of Texas as indicative of potential impairment (11.6 µg Chl $a \cdot L^{-1}$) (Texas Commission for Environmental Quality), and indices of eutrophication and water quality degradation such as the National Estuarine Eutrophication Assessment (20–60 µg Chl $a \cdot L^{-1}$; Bricker et al. 2003) and the National Coastal Condition Report produced by the US EPA (20 µg Chl $a \cdot L^{-1}$; https://www.epa.gov/national-aquatic-resource-surveys/national-coastal-condition-report-iv-2012). Overall, during the study period, Baffin Bay had a mean Chl a concentration (17.7 µg Chl $a \cdot L^{-1}$ $\pm$ 11.1) that was higher than many estuaries found around the world (see e.g., Cloern and Jassby 2008), including others along the US Gulf of Mexico coast (Pinckney et al. 2017; Geyer et al. 2018; Bugica et al. 2020). This, along with a trend of increasing Chl a and nutrients in the bay and watershed streams highlights that this waterbody is clearly undergoing eutrophication (Bricker et al. 2003; Wetz et al. 2017; Bugica et al. 2020).

In Baffin Bay, Chl a concentration exceeded the bloom threshold more frequently at high salinities (20% of high salinity Chl a observations were "blooms") compared to intermediate (5%) and low (6%) salinity conditions, while concentrations were statistically comparable at high and low salinities. These findings suggest that while blooms may be more frequent under high salinity conditions, overall, the system can support phytoplankton bloom development across a wide range of conditions, perhaps stimulated by different drivers based on species composition, such as salinity, flushing, and nutrient availability among others. For example, under low salinity conditions, some nutrients (phosphate, silicate) had relatively high concentrations compared to under high salinity conditions, while the nitrogen forms DON and ammonium were frequently high but did not show a pattern with Chl a. Previous work by Cira et al. (2021) estimated that residence times could be as short as ~3–4 weeks during these high rainfall/inflow periods,

which may be too short for some taxa to generate bloom level biomass (such as *A. lagunensis*; discussed later) but not for other taxa such as diatoms, which are able to rapidly respond to nutrient pulses. In contrast, during high salinity conditions, phosphate concentrations were generally lower than during wet conditions, but there was still considerable organic phosphorus, DON, and ammonium concentrations in the system. Previous work (Cotner et al. 2004; Wetz et al. 2017) and results shown here demonstrate that despite relatively high nitrogen to phosphorus ratios in both dissolved and particulate pools, indicating potential for phosphorus limitation, phytoplankton blooms are still common. This can be attributed to a combination of factors, namely, residence times that exceed one year (Montagna et al. 2018; Cira et al. 2021), efficient nutrient retention and cycling (An and Gardner 2002; Cotner et al. 2004; Wetz et al. 2017), and the unique ecophysiology of the dominant phytoplankton taxa during high salinity periods (*A. lagunensis*; discussed below). In general, these results are consistent with studies from other lagoonal estuaries showing that the combination of long residence time and regenerated nutrient availability can support phytoplankton growth and bloom development during periods of low inflow (Glibert et al. 2010; Hemraj et al. 2017; Barroso et al. 2018).

Widespread blooms at the beginning of this study's sampling period (at the end of a prolonged drought) were dominated by *A. lagunensis* (Cira and Wetz 2019), which historically flourishes at high salinities and long-residence times (Buskey et al. 2001; Cira and Wetz 2019; Cira et al. 2021). In addition, *A. lagunensis* is uniquely adapted to the potential for phosphorus-limiting conditions as well as a nutrient pool that is dominated by organic and/or reduced nutrient forms (e.g. Liu et al. 2001; Cotner et al. 2004; Agostoni and Erdner 2011; Gobler and Sunda 2012; Wetz et al. 2017). The Chl a at salinities exceeding ca. 45 and dominated by *A. lagunensis* coincided with both high DIN:DIP levels as well as a pattern of decreasing DON, potentially indicative of DON uptake by *A. lagunensis*. The 2013–2014 blooms of *A. lagunensis* consistently occurred during the warmest months of the year, emphasizing the warm water preference of this taxon (Gobler and Sunda 2012; Kang et al. 2017), and indicating a seasonal pattern for these blooms. Spring 2015 brought increasing precipitation and decreasing salinity, decreasing Chl a, and a gradual shift in phytoplankton abundance and composition. Five of the seven bloom measurements in 2015 were still dominated (> 50% of estimated biovolume) by *A. lagunensis* (Cira et al. 2021), despite the decreasing salinity. The other two blooms, one diatom and one chlorophyte/euglenoid dominated, occurred at low salinities (18 and 4, respectively). Many diatom taxa thrive in nutrient-replete, brackish conditions and cooler temperatures (Lavaud et al. 2007; Carstensen et al. 2015; Harding et al. 2015; Wilson et al. 2021). Chlorophyte and euglenoid taxa

tend to thrive at the freshwater end of estuarine continua (Leterme et al. 2015) and under intermediate to high nutrient conditions (Wehr et al. 2015; Graham et al. 2016); the BB1 site where blooms of these functional groups occurred often experienced increased NO$_x$ and/or orthophosphate concentrations with inflow events. Blooms in 2018 were observed in March and April at sites BB1 and BB2 at intermediate and high salinities and were again dominated by *A. lagunensis*. However, there was not the widespread monospecific bloom presence as in 2013 and 2014. *A. lagunensis* can resume vegetative growth from resting cells (Kang et al. 2017), and it is suspected the shallow tributary of Baffin Bay known as Laguna Salada (site BB2) may provide a protected reservoir for the species (Cira and Wetz 2019).

Subsequent rainfall and inflow events in 2018 resulted in flushing and a dramatic decrease in salinity throughout Baffin, preventing conditions conducive to further *A. lagunensis* bloom development and expansion. However, Chl *a* still reached bloom concentrations in late 2018 and early 2019, often dominated by diatoms, as well as chlorophytes/euglenoids (Jan 2019), and mixotrophic ciliates (*Mesodinium*, Feb 2019) (Chin et al. 2022). Likewise, the two blooms that occurred in summer 2021 followed substantial rain/inflow events and were dominated by diatoms and dinoflagellates. The lack of a clear, uniform set of drivers or correlational relationships with environmental variables suggests that varying drivers of phytoplankton biomass are in play across spatio-temporal scales (Brito et al. 2012; Pinckney et al. 2017; Geyer et al. 2018; Wilson et al. 2021), and highlights the need for additional studies employing higher frequency sampling, modeling and/or experimental approaches to fully elucidate the driving mechanism(s) behind blooms in this complex low-inflow estuary.

In addition to nutrient availability, light plays an important role in phytoplankton growth. In Baffin Bay, increased phytoplankton biomass contributes to reduced light penetration in the water column, consistent with high chlorophyll observations co-occurring lower Secchi depths. Unfortunately, with Secchi depth as the sole measure of light penetration, it is difficult to gauge the influence of light availability on phytoplankton dynamics in this study, given that the two parameters covary. More specific measures of underwater light conditions could be an informative area of future research for understanding overall controls of phytoplankton biomass in this system, as well as specific drivers of dominance by different groups. There were a small number of cases of density-driven stratification events, most often due to decreased surface water salinity following inflow events, but these did not consistently co-occur with elevated Chl *a* concentrations.

Over the past four decades, there has been a clear increase in the symptoms of eutrophication in Baffin Bay, many of which have had negative impacts on the ecosystem. Results presented here show that phytoplankton blooms can occur in all seasons and across the continuum of inflow conditions in Baffin Bay. The high phytoplankton biomass and bloom occurrence in Baffin Bay is consistent with findings from other low-inflow and/or lagoonal estuaries that demonstrate pronounced bloom potential and eutrophication symptoms, but with timing and conditions that can be difficult to characterize and predict compared to river-dominated systems. Results presented here and elsewhere (e.g. Cira et al. 2021) also show that long residence time, high salinity conditions tended to favor dominance of a single functional group, the harmful taxa *A. lagunensis*, while intermittent inflows act as a disturbance that can lead to a more diverse phytoplankton community (Barroso et al. 2018). Anticipated increases in regional temperature and drought are expected to create conditions under which *A. lagunensis* may further proliferate. On the other hand, extreme storm/precipitation events act as a disturbance, capable of flushing these populations out of the system before widespread blooms can occur. Reducing nutrient loads and maintaining strategic inflow targets to Baffin Bay are likely to be important management strategies to curbing future *A. lagunensis* blooms.

Declarations

References

Agostoni, M., and D.L. Erdner. 2011. Analysis of ammonium transporter and urease gene expression in Aureoumbra lagunensis. *Harmful Algae* 10: 549–556. https://doi.org/10.1016/J.HAL.2011.04.007.

An, S., and W.S. Gardner. 2002. Dissimilatory nitrate reduction to ammonium (DNRA) as a nitrogen link, versus denitrification as a sink in a shallow estuary (Laguna Madre/Baffin Bay, Texas). *Marine Ecology Progress Series* 237: 41–50. https://doi.org/10.3354/meps237041.

Barbier, E.B., S.D. Hacker, C. Kennedy, E.W. Koch, A.C. Stier, and B.R. Silliman. 2011. The value of estuarine and coastal ecosystem services. *Ecological Monographs* 81: 169–193.

Barroso, H.D.S., T.C.L. Tavares, M.D.O. Soares, T.M. Garcia, B. Rozendo, A.S.C. Vieira, P.B. Viana, et al. 2018. Intra-annual variability of phytoplankton biomass and nutrients in a tropical estuary during a severe drought. *Estuarine, Coastal and Shelf Science* 213: 283–293. https://doi.org/10.1016/j.ecss.2018.08.023.

Boyer, J.N., C.R. Kelble, P.B. Ortner, and D.T. Rudnick. 2009. Phytoplankton bloom status: Chlorophyll a biomass as an indicator of water quality condition in the southern estuaries of Florida, USA. *Ecological Indicators*. https://doi.org/10.1016/J.ECOLIND.2008.11.013.

Bricker, S.B., J.G. Ferreira, and T. Simas. 2003. An integrated methodology for assessment of estuarine trophic status. *Ecological Modelling* 169: 39–60. https://doi.org/10.1016/S0304-3800(03)00199-6.

Bricker, S.B., B. Longstaff, W. Dennison, A. Jones, K. Boicourt, C. Wicks, and J. Woerner. 2008. Effects of nutrient enrichment in the nation's estuaries: A decade of change. *Harmful Algae* 8: 21–32. https://doi.org/10.1016/j.hal.2008.08.028.

Brito, A.C., T. Quental, T.P. Coutinho, M.A.C. Branco, M. Falcão, A. Newton, J. Icely, and T. Moita. 2012. Phytoplankton dynamics in southern Portuguese coastal lagoons during a discontinuous period of 40 years: An overview. *Estuarine, Coastal and Shelf Science* 110: 147–156. https://doi.org/10.1016/j.ecss.2012.04.014.

Bugica, K., B. Sterba-Boatwright, and M.S. Wetz. 2020. Water quality trends in Texas estuaries. *Marine Pollution Bulletin* 152: 110903. https://doi.org/10.1016/j.marpolbul.2020.110903.

Buskey, E.J., and C.J. Hyatt. 1995. Effects of the Texas (USA) "brown tide" alga on planktonic grazers. *Marine Ecology Progress Series* 126: 285–292. https://doi.org/10.3354/meps126285.

Buskey, Edward J., H. Liu, C. Collumb, and J.G.F. Bersano. 2001. The decline and recovery of a persistent Texas brown tide algal bloom in the Laguna Madre (Texas, USA). *Estuaries* 24: 337–346. https://doi.org/10.2307/1353236.

Carstensen, J., P. Henriksen, and A.-S. Heiskanen. 2007. Summer algal blooms in shallow estuaries: Definition, mechanisms, and link to eutrophication. *Limnology and Oceanography* 52: 370–384.

Carstensen, J., R. Klais, and J.E. Cloern. 2015. Phytoplankton blooms in estuarine and coastal waters: Seasonal patterns and key species. *Estuarine, Coastal and Shelf Science* 162: 98–109. https://doi.org/10.1016/j.ecss.2015.05.005.

Chin, T., L. Beecraft, and M. Wetz. 2022. Phytoplankton biomass and community composition in three Texas estuaries differing in

freshwater inflow regime. *Estuarine, Coastal and Shelf Science* 277: 108059. https://doi.org/10.1016/J.ECSS.2022.108059.

Cira, E.K., and M.S. Wetz. 2019. Spatial-temporal distribution of Aureoumbra lagunensis ("brown tide") in Baffin Bay, Texas. *Harmful Algae* 89: 101669. https://doi.org/10.1016/j.hal.2019.101669.

Cira, E.K., T.A. Palmer, and M.S. Wetz. 2021. Phytoplankton dynamics in a low-inflow estuary (Baffin Bay, TX) during drought and high-rainfall conditions associated with an El Niño event. *Estuaries and Coasts* 44: 1752–1764. https://doi.org/10.1007/s12237-021-00904-7/Published.

Cloern, J.E., and A.D. Jassby. 2008. Complex seasonal patterns of primary producers at the land-sea interface. *Ecology Letters* 11: 1294–1303. https://doi.org/10.1111/J.1461-0248.2008.01244.X.

Cotner, J.B., M.W. Suplee, N.W. Chen, and D.E. Shormann. 2004. Nutrient, sulfur and carbon dynamics in a hypersaline lagoon. *Estuarine, Coastal and Shelf Science* 59: 63–652. https://doi.org/10.1016/j.ecss.2003.11.008.

Geyer, N.L., M. Huettel, and M.S. Wetz. 2018. Phytoplankton spatial variability in the river-dominated estuary, Apalachicola Bay, Florida. *Estuaries and Coasts* 41: 2024–2038. https://doi.org/10.1007/s12237-018-0402-y.

Glibert, P.M., J.N. Boyer, C.A. Heil, C.J. Madden, B. Sturgis, and C.S. Wazniak. 2010. Blooms in lagoons: Different from those of river-dominated estuaries. In *Coastal lagoons: critical habitats of environmental change*, ed. M.J. Kennish and H.W. Paerl. CRC Press.

Gobler, C.J., and W.G. Sunda. 2012. Ecosystem disruptive algal blooms of the brown tide species, *Aureococcus anophagefferens* and *Aureoumbra lagunensis*. *Harmful Algae* 14: 36–45. https://doi.org/10.1016/j.hal.2011.10.013.

Graham, L.E., J.M. Graham, L.W. Wilcox, and M.E. Cook. 2016. *Algae*, 3rd ed. LJLM Press.

Harding, L.W., J.E. Adolf, M.E. Mallonee, W.D. Miller, C.L. Gallegos, E.S. Perry, J.M. Johnson, K.G. Sellner, and H.W. Paerl. 2015. Climate effects on phytoplankton floral composition in Chesapeake Bay. *Estuarine, Coastal and Shelf Science* 162: 53–68. https://doi.org/10.1016/j.ecss.2014.12.030.

Hemraj, D.A., M.A. Hossain, Q. Ye, J.G. Qin, and S.C. Leterme. 2017. Plankton bioindicators of environmental conditions in coastal lagoons. *Estuarine, Coastal and Shelf Science* 184: 102–114. https://doi.org/10.1016/J.ECSS.2016.10.045.

Kang, Y., Y.Z. Tang, G.T. Taylor, and C.J. Gobler. 2017. Discovery of a resting stage in the harmful, brown-tide-causing pelagophyte, Aureoumbra lagunensis: A mechanism potentially facilitating recurrent blooms and geographic expansion. *Journal of Phycology* 53: 118–130. https://doi.org/10.1111/JPY.12485.

Kassambara, A. 2020. rstatix: Pipe-friendly framework for basic statistical tests. R package version 0.7.0. https://CRAN.R-project.org/package=rstatix.

Kloesel, K., B. Bartush, J. Banner, D. Brown, J. Lemery, X. Lin, C. Loeffler, et al. 2018. Impacts, risks, and adaptation in the United States - Southern Great Plains. In *Fourth National Climate Assessment*, vol. 2. U.S. Global Change Research Program. https://doi.org/10.7930/NCA4.2018.CH23.

Knoppers, B., B. Kjerfve, and J.-P. Carmouze. 1991. Trophic state and water turn-over time in six choked coastal lagoons in Brazil. *Biogeochemistry* 14: 149–166.

Largier, J. 2010. Low-inflow estuaries: hypersaline, inverse, and thermal scenarios. In Contemporary Issues in Estuarine Physics, ed. A. Valle-Levinson, 247–272. Cambridge: Cambridge University Press.

Lavaud, J., R.F. Strzepek, and P.G. Kroth. 2007. Photoprotection capacity differs among diatoms: Possible consequences on the spatial distribution of diatoms related to fluctuations in the underwater light climate. *Limnology and Oceanography* 52: 1188–1194. https://doi.org/10.4319/lo.2007.52.3.1188.

Lemley, D.A., J.B. Adams, and N.A. Strydom. 2017. Testing the efficacy of an estuarine eutrophic condition index: Does it account for shifts in flow conditions? *Ecological Indicators* 74: 357–370. https://doi.org/10.1016/J.ECOLIND.2016.11.034.

Lemley, D.A., S.J. Lamberth, W. Manuel, M. Nunes, G.M. Rishworth, L. van Niekerk, and J.B. Adams. 2021. Effective management of closed hypereutrophic estuaries requires catchment-scale interventions. *Frontiers in Marine Science* 8: 1–17. https://doi.org/10.3389/fmars.2021.688933.

Leterme, S.C., L. Allais, J. Jendyk, D.A. Hemraj, K. Newton, J. Mitchell, and M. Shanafield. 2015. Drought conditions and recovery in the Coorong wetland, south Australia in 1997–2013. *Estuarine, Coastal and Shelf Science* 163: 175–184. https://doi.org/10.1016/J.ECSS.2015.06.009.

Liu, H., E.A. Laws, T.A. Villareal, and E.J. Buskey. 2001. Nutrient-limited growth of Aureoumbra lagunensis (Pelagophyceae), with implications for its capability to outgrow other phytoplankton species in phosphate-limited environments. *Journal of Phycology* 37: 500–508. https://doi.org/10.1046/J.1529-8817.2001.037004500.X.

McCune, B., and M.J. Mefford. 2018. *PC-ORD. Multivariate analysis of ecological data. Version 7.08*. Corvallis, Oregon, U.S.A.: Wild Blueberry Media.

Montagna, P.A., X. Hu, T.A. Palmer, and M. Wetz. 2018. Effect of hydrological variability on the biogeochemistry of estuaries across a regional climatic gradient. *Limnology and Oceanography* 63: 2465–2478. https://doi.org/10.1002/lno.10953.

Nielsen-Gammon, J.W., J.L. Banner, B.I. Cook, D.M. Tremaine, C.I. Wong, R.E. Mace, H. Gao, et al. 2022. Unprecedented drought challenges for Texas water resources in a Changing climate: What do researchers and stakeholders need to know? *Earth's Future* 8: e2020EF001552. https://doi.org/10.1029/2020EF001552.

Onuf, C.P. 1996. Seagrass responses to long-term light reduction by brown tide in upper Laguna Madre, Texas: Distribution and biomass patterns. *Marine Ecology Progress Series* 138: 219–231. https://doi.org/10.3354/meps138219.

Pendleton, L. 2010. *The economic and market value of coasts and estuaries: What's at stake?* Restore America's estuaries.

Pereira Coutinho, M.T., A.C. Brito, P. Pereira, A.S. Gonçalves, and M.T. Moita. 2012. A phytoplankton tool for water quality assessment in semi-enclosed coastal lagoons: Open vs closed regimes. *Estuarine, Coastal and Shelf Science* 110: 134–146. https://doi.org/10.1016/J.ECSS.2012.04.007.

Pinckney, J.L., A.S. Quigg, and D.L. Roelke. 2017. Interannual and seasonal patterns of estuarine phytoplankton diversity in Galveston Bay, Texas, USA. *Estuaries and Coasts* 40: 310–316. https://doi.org/10.1007/s12237-016-0135-8.

R Core Team. 2020. *R: A language and environment for statistical computing*. Vienna, Austria: R Foundation for Statistical Computing.

Scanes, E., P.R. Scanes, and P.M. Ross. 2020. Climate change rapidly warms and acidifies Australian estuaries. *Nature Communications* 11: 1–11. https://doi.org/10.1038/s41467-020-15550-z.

Scavia, D., and Y. Liu. 2009. Exploring estuarine nutrient susceptibility. *Environmental Science and Technology* 43: 3474–3479. https://doi.org/10.1021/es803401y.

Seneviratne, S.I., N. Nicholls, D. Easterling, C.M. Goodess, S. Kanae, J. Kossin, Y. Luo, et al. 2012. Changes in climate extremes and their impacts on the natural physical environment. In *Managing the Risks of Extreme Events and Disasters to Advance Climate Change Adaptation: Special Report of the Intergovernmental Panel on Climate Change*, vol. 9781107025, 109–230. Cambridge University Press. https://doi.org/10.1017/CBO9781139177245.006.

Smayda, T.J. 1997. What is a bloom? A commentary. *Limnology & Oceanography* 42: 1132–1136.

Street, G.T., P.A. Montagna, and P.L. Parker. 1997. Incorporation of brown tide into an estuarine food web. *Marine Ecology Progress Series* 152: 67–78.

Tolan, J.M. 2007. El Niño-Southern Oscillation impacts translated to the watershed scale: Estuarine salinity patterns along the Texas Gulf Coast, 1982 to 2004. *Estuarine, Coastal and Shelf Science* 72: 247–260. https://doi.org/10.1016/J.ECSS.2006.10.018.

Tunnell, J.W., and F.W. Judd. 2002. The Laguna Madre of Texas and Tamaulipas. 1st ed. Gulf Coast Studies, No. 2. College Station: Texas A & M University Press.

U.S. EPA. 2000. *Nutrient criteria technical guidance manual lakes and reservoirs*. Washington, DC.

Wehr, J., R. Sheath, and J.P. Kociolek. 2015. *Freshwater Algae of North America*. Academic Press.

Wetz, M.S., E.K. Cira, B. Sterba-Boatwright, P.A. Montagna, T.A. Palmer, and K.C. Hayes. 2017. Exceptionally high organic nitrogen concentrations in a semi-arid South Texas estuary susceptible to brown tide blooms. *Estuarine, Coastal and Shelf Science* 188: 27–37. https://doi.org/10.1016/j.ecss.2017.02.001.

Wickham, H., M. Averick, J. Bryan, W. Chang, L.D.A. Mcgowan, R. François, et al. 2019. Welcome to the Tidyverse. *Journal of Open Source Software* 4: 1686. https://doi.org/10.21105/joss.01686.

Wilson, J.R., F.P. Wilkerson, S.B. Blaser, and K.J. Nielsen. 2021. Phytoplankton community structure in a seasonal low-inflow estuary adjacent to coastal upwelling (Drakes Estero, CA, USA). *Estuaries and Coasts* 44: 769–787. https://doi.org/10.1007/s12237-020-00792-3.